RSC Advances

ROYAL SOCIETY OF CHEMISTRY

www.rsc.org/advances

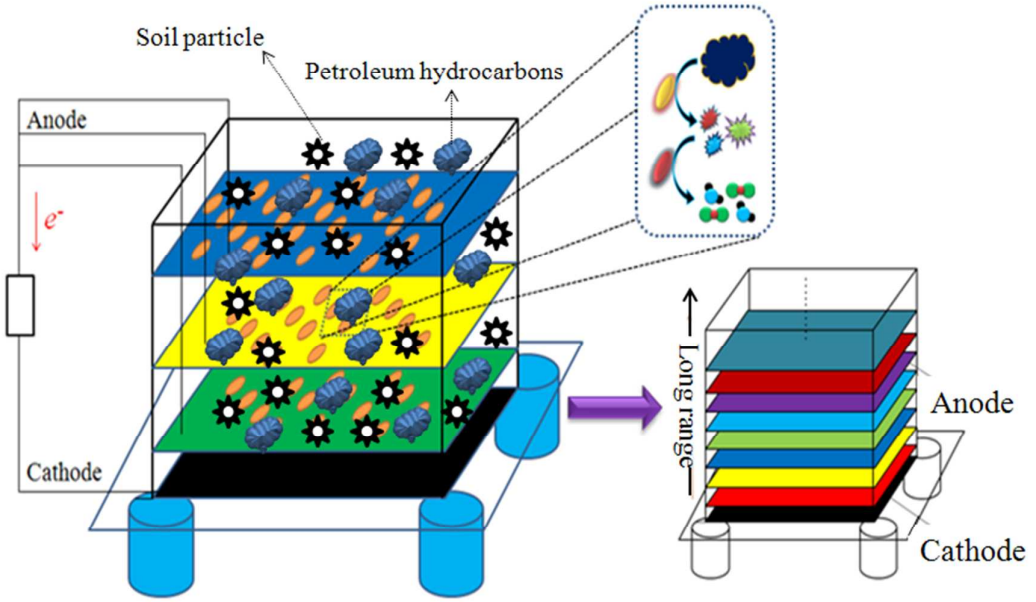

More Coulomb and higher degradation rate of hydrocarbons in soil are obtained using a multi-anode bioelectrochemical system.

Date: September 17, 2014
Draft for: *RSC Advances*
Research Article

Extended Petroleum Hydrocarbon Bioremediation in Saline Soil Using Pt-free Multianodes Microbial Fuel Cells

Xiaojing Li, Xin Wang*, Yueyong Zhang, Lijuan Cheng, Jie Liu, Fan Li, Bingli Gao and Qixing Zhou*

MOE Key Laboratory of Pollution Processes and Environmental Criteria / Tianjin Key Laboratory of Environmental Remediation and Pollution Control / College of Environmental Science and Engineering, Nankai University, No. 94 Weijin Road, Nankai District, Tianjin 300071, China

*Corresponding Authors: Phone: (86)22-23507800; fax: (86)22-23501117; E-mail: zhouqx@nankai.edu.cn (Zhou Q.); xinwang1@nankai.edu.cn (Wang X.)

Abstract: Bioelectrochemical remediation is an emerging technology for *in-situ* removal of petroleum hydrocarbons in soil. Here we demonstrated that the remediation can be extended to a larger range by adding multilayer anodes in contaminated soils. Using a three anodes system with only one activated carbon as the cathodic catalyst, 918 C of charge transferred during 180 days in aged saline soil. The degradation of both polycyclic aromatic hydrocarbons (PAHs) and *n*-alkanes were accelerated in each layer compared to the disconnected control. The net degradation rates of total petroleum hydrocarbons, 16 priority PAHs and total *n*-alkanes (C8–C40) were 18%, 36% and 29%, respectively. Popular exoelectrogenes (such as *Geobacteraceae* sp.) and *Escherichia* were identified, which possibly played an important role in this bioelectrochemical process.

Introduction

The petroleum is one of dominant energy sources to promote the economic and social development of a country. However, large amounts of petroleum hydrocarbons had been leaked to the environment during the exploration, extraction, refining, transportation and processing [1]. Many countries and regions are suffering from the ecological risk from soil contamination of petroleum hydrocarbons [2, 3]. The regular remediation approaches for petroleum contamination in soil mainly include physical, chemical and biological technologies [4]. Since the physical and chemical remediations are usually expensive and might cause secondary pollution [5], the bioremediation, including bioaugmentation and biostimulation, is a green and cost-effective technology.

Different from the common biotechnologies, the microbial fuel cell (MFC) is a new technology that can be used to remove organic pollutants through the bio-generated current to remediate water [6-8], sediment [9-11] or soil [12, 13]. Since the electron acceptor is non-exhaustible and passively applied, the air-cathode MFC has its advantage in potential use of real remediation. Our early studies showed that the degradation rate of total petroleum hydrocarbon (TPH) had been enhanced by 120% in soil close to the anode (< 1 cm) at water saturated condition (33% moisture content) [13]. The maximum degradation rates of C8–C40 and 16 polycyclic aromatic hydrocarbons (PAHs) reached 79% and 42% respectively, with charge output of 125±7 C at the end of the experiment (25 d, with additional nutrient amendment) [13].

Previous reports indicated that the degradation rates of hydrocarbons decreased with the increase of distance to the anode using sandwiched anode-separator-cathode systems and 1 cm of distance was optimal [13, 14]. In these systems, the areas of anode and cathode are nearly the same. It should be noted that the maximum current density of soil MFCs (~80 $mA \cdot m^{-2}$, 1000 Ω) was 10 times lower than those of MFCs (~800 $mA \cdot m^{-2}$, 1000 Ω) used in water [15], indicating that the cathode with a fixed area can afford a much larger anode in soil than in water. To extend the anode in soil and test the possibility of long range bioremediation, in this study, anodes were inserted parallelly with different distance from the air-cathode in petroleum hydrocarbon contaminated soil. The characteristics and the degradation rates of C8–C40 and 16 PAHs as well as bacterial communities in soils were investigated. Furthermore, Pt was substituted by activated carbon (AC) as the cathodic catalyst in soil MFCs for

bioremediation.

Results and discussion

Performance of SMFC

For each SMFC, three anodes were parallelly inserted with distances of 1, 3 and 5 cm to the cathode since the degradation of hydrocarbons in soils less than 1 cm to the anode can be accelerated [13]. After filling soil into the SMFC with multilayer anodes, the voltage initially increased and then decreased throughout the experimental period (Figure 2). The maximum power density of 37 $mW \cdot m^{-2}$ (366 mV, 102 $mA \cdot m^{-2}$, across 1000 Ω resistor) was achieved on day 5, with a comparable value as previously reported (39 $mW \cdot m^{-2}$, across 100 Ω resistor using Pt/C cathode) [14]. The voltage exhibited a sharp decline during 6–10 days, probably due to the depletion of easily degraded substrate. [16] The voltage then slowly decreased until the end of experiment, which can be attributed to the degradation of relatively recalcitrant compounds (such as PAHs). Over the tested period (about 180 days), the accumulated charge reached 918 C (Figure 2), with a value 7 times higher than our previous result, indicating that the extension of anode enabled the SMFC to collect electrons from a larger range of soil. The average charge output rate during 180 days was 5.1 $C \cdot d^{-1}$, which was consistent with that (5 $C \cdot d^{-1}$, using Pt catalyst) previously reported by us in a much shorter period (25 days) [13].

Changes in characteristics of soils

In the connected SMFC, the soil pH gradually increased with the decrease of distance to the air-cathode (Figure S1a). The highest pH of 9.28±0.01 was observed in the SL4,

which was 12 % higher than 8.26±0.12 in the disconnected control (here we marked it as natural attenuation, NA). In the connected SMFC, the pH of SL3 (9.02±0), SL2 (9.02±0.04) and SL1 (8.92±0.07) were 9 %, 9 % and 8 % higher than that of the NA. The pH of mixed soil from four layers (mixed) also increased by 0.85 unit compared to NA. The increase of pH can be attributed to the accumulation of hydroxyl close to the air-cathode [17] or bicarbonate accumulation resulted from biodegradation of hydrocarbon [14]. Such an alkaline condition could enhance the bioavailability of hydrocarbon and thus facilitate electricity generation with simultaneous pollutant removal [18].

The increase of soil pH may incur a precipitation of some metal ions (such as Ca^{2+} and Mg^{2+}) and restrict the transport of ions. As an evidence, the soil conductivity, a parameter showing the soluble ions that can be freely transferred in soil cracks, decreased from SL1 to SL3 except the SL4 (Figure S1b). The obvious increase of conductivity at SL4 can be resulted from the water evaporation through the air-cathode so that the supplementary downward flow carrying ions so that these ions accumulated at the bottom of the reactor (SL4). Compared to the NA, the conductivity of mixed soils from all layers decreased by 16%, probably due to the increase of soil pH as interpreted above.

Degradation of petroleum hydrocarbons

The concentrations of TPHs in each layer were analyzed after 180 days. As showed in Figure S2, the net degradation rates of TPH decreased as follow: SL4 (18±0.4%) > SL1 (13±0.2%) > SL2 (10±0.0%) > SL3 (8±0.2%). The net degradation rate of TPH

in mixed soil (SL1 to SL 4) was only 12±0.0 % because we used an aged petroleum hydrocarbon contaminated soil (see below) [19] with a high salinity [20].

The dominant PAHs were phenanthrene (Phe, C14), fluoranthene (Flu, C16), pyrene (Pyr, C16) and chrysene (Chr, C18), accounting for 72% of total PAHs in NA (Figure 3a). The net degradation rates of PAHs were ranged from 20% to 72% except Chr of 7%, Fluorene (Fln, C13) of 4%, Dibenz(ah)anthracene (DahA, C22) of –10% and Benzo(ghi)perylene (BghiP, C22) of –3%. The net degradation rate of total PAHs (sum of 16 PAHs) in mixed soil was 27±4% with the values decreased from 5653 to 4146 $ng \cdot g^{-1}$, where the degradation of three dominant PAHs accounted for 70%. The total PAHs net degradation rates in each layer decreased as: SL4 (36±9%) > SL1 (27±7%) > SL2 (19±5%) > SL3 (14±4%), following a similar trend as the net degradation rates of TPHs (Figure 3b).

Dominant components of *n*-alkanes (C8-C40) dropped in the range of C16–C38 (Figure 4), suggesting that the petroleum hydrocarbons in this soil were well aged, which was also demonstrated by the considerable contents of pristane (30 $\mu g \cdot g^{-1}$) and phytane (169 $\mu g \cdot g^{-1}$) in NA. The concentration of total *n*-alkanes (sum of C8–C40) in mixed soils decreased by 29±5% from 609 to 434 $\mu g \cdot g^{-1}$. The highest degradation rates were all obtained on C13 (the first peak in Figure 4) in both mixed and layered soils, with the highest value of 85±3% observed in SL3. The other peak of net degradation rate reached 33–41% on C34–C36 (Figure 4). The net degradation rates of C8–C40 in layered soils were SL1 (32±10%) > SL4 (29±15%) > SL2 (20±6%) > SL3 (19±3%), showing a partly similar trend as those of TPHs. Differently, the

highest degradation rate was observed in the layer close to air-cathode (SL4), probably due to the increased bioavailability of *n*-alkanes by the high pH.

Microbial communities

As showed by DGGE profiles of the disconnected control (NA) and SMFC operated at 1000 Ω (CC) over 180 days, the internal and outside charge transfer in SMFCs affected the microbial community (Figure 5). Bands 1, 3 and 12 were present in CC but poorly visible in NA, while bands 5 and 6 were only noticed in NA. Moreover, both the Shannon-Wiener Index (*H*) and Richness (*S*) of CC (3.39 and 39) were higher than those of NA (3.35 and 37, Figure 5b), indicating the microbial community in soil was indeed stimulated by the current. However, the Uniformity Index (E_H) of CC showed a slightly low value of 0.926 compared to 0.928 of NA, indicating a selective enrichment of specific communities [14]. The results of clone sequencing exhibited that the majority of the amplified clones derived from the SMFC belongs to γ-*Proteobacteria* [14, 21] (Table 1). *Alcanivorax* sp. was detected in band 13 as a hydrocarbon degradation bacteria, which was obviously enhanced in SMFC by the stimulation of bio-generated current, indicating that the bioelectricity has a solid contribution on stimulating the growth of hydrocarbon degradation bacteria. Furthermore, two species of *Firmicutes* (band 3 and 4) that potentially associated with hydrocarbon degradation were also observed in both NA and CC [14]. Uncultured *Geobacteraceae* sp. in band 2 was the possible exoelectrogenic bacteria in this system [22]. Several species of *Escherichia* sp. were found in soil samples. These bacteria could play an important role on electron transfer between the electrode and the microbial

community in soil (such as producing soluble excretions) [23, 24]. The real functions of these bacteria should be confirmed by defined binary culture in the future.

Conclusions

It had been demonstrated in this study that the bioelectrochemical remediation of petroleum hydrocarbons in soil can be extended to a larger range using multilayer anodes. Using activated carbon as the cathodic catalyst, the charge output reached 918 C at 1000 Ω. Soil pH was increased during the remediation, especially the soil close to the cathode. The degradation of both PAHs and *n*-alkanes were accelerated by the bioelectrochemical process. The *Geobacteraceae* sp. and *Escherichia* sp. were found in this system, possibly played a key role in electricity generation and petroleum hydrocarbons degradation.

Experimental

Saline soil

Saline soil contaminated by petroleum hydrocarbon was excavated from the ground surface (<10 cm in depth) around beam balanced pumping units in Dagang Oilfield (Tianjin, China). The soil was partially air-dried and passed through 2 mm sieve. After mixing, the sieved soil was analyzed for properties (Table S1).

According to our early studies, the saturated water content in soil substantially enhanced the degradation of hydrocarbons and the number of hydrocarbon degradation bacteria [13]. Thus, all the experiments here were employed under a water layer (waterlogged) to facilitate the diffusion of proton/hydroxide and keep a good

171 anaerobic environment.

172 **MFC configuration and operation**

173 A soil MFC (SMFC, 6 cm × 6 cm × 9 cm) was designed with three layers of anodes
174 parallelly inserted in the soil and an AC air-cathode at the bottom as illustrated in
175 Figure 1a. Anodes were made of carbon meshes (6 × 6 cm, Jilin Carbon Factory, Jilin,
176 China). Carbon meshes were soaked in acetone overnight and rinsed in water for three
177 times before using [25]. AC air-cathodes (6 × 6 cm, 60 × 60 stainless steel mesh) were
178 made by rolling-press method according to previous descriptions [26, 27]. The catalyst
179 layer was directly contacted with the soil, while the gas diffusion layer on the
180 opposite side was exposed to the air. The cathode was fixed by a porous Plexiglas
181 plate (pore diameter of 0.5 cm, with a spacing of 1 cm between two pores, Figure 1b)
182 at the bottom of SMFC.

183 340 g of contaminated dry soil was equably mixed with 90 mL distilled water and
184 filled into two identical SMFCs. For each SMFC, three anodes were parallelly
185 inserted with distances of 1 cm (Layer 3), 3 cm (Layer 2) and 5 cm (Layer 1) to the
186 cathode before the reactor was sealed with distilled water. Titanium sheet with 1 cm in
187 width and 1 mm in thickness was firmly fixed at the edges of each electrode as the
188 current collector (Figure 1b). One SMFC was operated at open circuit condition as the
189 control, and the other SMFC was operated with all anodes connected together to the
190 cathode through a 1000 Ω external resistance in a 30 °C constant temperature
191 incubator. At the end of the test, soil samples between electrodes were obtained and
192 marked as SL1, SL2, SL3, SL4 for analysis (Figure 1b).

193 **Chemical and electrochemical analysis**

194 TPH, *n*-alkanes and 16 priority PAHs were measured according to the procedures
195 described previously [13]. The net degradation rate was calculated as
196 $\eta = (C_{NA} - C)/C_{NA}$, where C_{NA} is the pollutant (such as PAH) concentration in the
197 disconnected control reactor and C is the concentration of the same pollutant in the
198 connected SMFC. The overall net degradation rate of PAHs (or 33 *n*-alkanes) was
199 calculated by the summing concentrations of 16 PAHs (or 33 *n*-alkanes) up. Soil
200 samples taken from each layer and the uniform mixture of all soils (mixed) were
201 prepared to measure concentrations of TPHs, PAHs and *n*-alkanes.

202 The pH and conductivity of soil were measured in a mixture of soil and distilled
203 water with a weight (2 g) / volume (10 mL) ratio of 1:5. Available nitrogen, available
204 phosphorus, available potassium and organic matter was determined by conventional
205 methods [28]. The contents of Zn, Cu, Ni, Mn, Fe, Pb, Cr, Cd were extracted by
206 microwave digestion method and measured using ICP-OES (Vista MPX Varian, US)
207 [29].

208 Voltages (U, mV) across 1000 Ω external resistance (R, Ω) were recorded every
209 1800 s (t) using a data acquisition system (PISO-813, ICP DAS Co., Ltd, Shanghai,
210 China). The power densities (P, $mW \cdot m^{-2}$) were normalized to the cathodic projected
211 area (A = 0.0036 m^{-2}) and calculated as $P = U^2/(RA)$ [30]. Total charge output was
212 obtained by $Q = \int_0^T (U/R)dt$, where T (s) is the cycle time.

213 **Biological analysis**

214 Bacterial genomic DNA was extracted from the soil sample using the DNA Gel

Extraction Kit (OMEGA, US) according to the instructions of manufacturer. The universal primer set GC-338F (5′-CGC CCG GGG CGC GCC CCG GGG CGG GGC GGG GGC GCG GGG GG CCT ACG GGA GGC AGC AG-3′) and 518R (5′-ATT ACC GCG GCT GCT GG-3′) was used to amplify the V3 region of bacterial 16S rDNA. PCR amplification was performed in T-gradient (Biometra, GER) under the following conditions: initial denaturation at 94 °C for 5 min, denaturation at 94 °C for 1 min, renaturation at 55 °C for 45 s, extension at 72 °C for 1 min, followed by 30 cycles and finally at 72 °C for 10 min.

Denaturing gradient gel electrophoresis (DGGE) was performed using the Gel-Doc 2000 (Bio-Rad, US). PCR products (10 μL) were loaded onto 8% polyacrylamide gels containing a gradient of denaturant ranging from 35% to 55% (100% corresponded to 7 M urea and 40% *vt*% acrylamide). DGGE was run in 1×TAE buffer at 150 V for 5 h (60 °C). After electrophoresis, the gels were stained as the process of argentation dyeing (15 min) before being photographed. Bands of interest were excised and recovered using the Poly-Gel DNA Extraction Kit (OMEGA, US).

The PCR products were verified using a 1.2 % agarose gel and then sent for sequencing after re-amplified PCR (Genia Biological Technology Co., Ltd., Beijing, China). The sequences were compared with those of the NCBI BLAST GenBank nucleotide sequence databases and the BLAST program (http://www.ncbi.nlm.nih.gov/BLAST/).

Quantity One was used to analyze DGGE pattern, and Shannon-Wiener Index (*H*),

Uniformity Index (E_H) and Richness (S) was calculated by Origin. $H = -\sum(N_i/N \ln(N_i/N))$, where N_i is the optical density of the band i and N is the sum of optical density of all bands. $E_H = H/\ln S$, where S is the number of the band [31].

Acknowledgments

The authors thank Dr. Yuan Lu for help with the GC-MS analysis. This research work was financially supported by MOE Innovative Research Team in University (IRT13024), the Ministry of Science and Technology as an 863 major project (grant No. 2013AA06A205), the National Natural Science Foundation of China as a young scholar project (No. 21107053) and as a key project (No. 21037002), the Fundamental Research Funds for the Central Universities and the Ph.D. Candidate Research Innovation Fund of Nankai University (No. 68140001).

References

1. M. Ayotamuno, R. Kogbara, S. Ogaji and S. Probert, *Applied energy*, 2006, **83**, 1249-1257.
2. C. Hall, P. Tharakan, J. Hallock, C. Cleveland and M. Jefferson, *Nature*, 2003, **426**, 318-322.
3. Q. Zhou, F. Sun and R. Liu, *Environment international*, 2005, **31**, 835-839.
4. Q. Zhou and Y. Song, *Principles and methods of contaminated soil remediation*, Science Press, Beijing, China, 2004.
5. E. Riser-Roberts, *Remediation of petroleum contaminated soils: biological, physical, and chemical processes*, CRC Press, 1998.
6. J. M. Morris and S. Jin, *Journal of environmental science and health. Part A*, 2008, **43**, 18-23.
7. J. M. Morris, S. Jin, B. Crimi and A. Pruden, *Chemical Engineering Journal*, 2009, **146**, 161-167.
8. P. Liang, J. Wei, M. Li and X. Huang, *Frontiers of Environmental Science & Engineering*, 2013, **7**, 913-919.
9. J. M. Morris and S. Jin, *Journal of hazardous materials*, 2012, **213**, 474-477.
10. Y. Yuan, S. Zhou and L. Zhuang, *Journal of Soils and Sediments*, 2010, **10**, 1427-1433.
11. A. Wang, H. Cheng, N. Ren, D. Cui, N. Lin and W. Wu, *Frontiers of Environmental Science & Engineering*, 2012, **6**, 569-574.
12. D. Huang, S. Zhou, Q. Chen, B. Zhao, Y. Yuan and L. Zhuang, *Chemical Engineering Journal*, 2011, **172**, 647-653.
13. X. Wang, Z. Cai, Q. Zhou, Z. Zhang and C. Chen, *Biotechnology and bioengineering*, 2012, **109**, 426-433.

14. L. Lu, T. Huggins, S. Jin, Y. Zuo and Z. J. Ren, *Environmental science & technology*, 2014, **48**, 4021-4029.
15. X. Liu, W. Li and H. Yu, *Chemical Society Reviews*, 2014.
16. L. Lu, H. Yazdi, S. Jin, Y. Zuo, P. H. Fallgren and Z. J. Ren, *Journal of Hazardous Materials*, 2014, **274**, 8-15.
17. X. Wang, C. Feng, N. Ding, Q. Zhang, N. Li, X. Li, Y. Zhang and Q. Zhou, *Environmental science & technology*, 2014, **48**, 4191-4198.
18. Y. Yuan, Q. Chen, S. Zhou, L. Zhuang and P. Hu, *Journal of Chemical Technology and Biotechnology*, 2012, **87**, 80-86.
19. J. Tang, X. Lu, Q. Sun and W. Zhu, *Agriculture, Ecosystems & Environment*, 2012, **149**, 109-117.
20. X. Qin, D. Li, J. Tang, Q. Zhang and J. Gao, *Letter in applied microbiology*, 2012, **55**, 210-217.
21. B. E. Logan, *Nature Reviews Microbiology*, 2009, **7**, 375-381.
22. D. R. Lovley, *Nature Reviews Microbiology*, 2006, **4**, 497-508.
23. Y. Wang, S. Tsujimura, S. Cheng and K. Kano, *Applied microbiology and biotechnology*, 2007, **76**, 1439-1446.
24. T. Zhang, C. Cui, S. Chen, H. Yang and P. Shen, *Electrochemistry communications*, 2008, **10**, 293-297.
25. X. Wang, S. Cheng, Y. Feng, M. D. Merrill, T. Saito and B. E. Logan, *Environmental science & technology*, 2009, **43**, 6870-6874.
26. H. Dong, H. Yu, H. Yu, N. Gao and X. Wang, *Journal of Power Sources*, 2013, **232**, 132-138.
27. X. Li, X. Wang, Y. Zhang, N. Ding and Q. Zhou, *Applied Energy*, 2014, **123**, 13-18.
28. G. Liu, *Soil physical and chemical analysis and description of soil profiles*, China Standard Press, Beijing, China, 1996.
29. Y. Sun, Q. Zhou, X. Xie and R. Liu, *Journal of hazardous materials*, 2010, **174**, 455-462.
30. Y. Zhang, X. Wang, X. Li, N. Gao, L. Wan, C. Feng and Q. Zhou, *RSC Advances*, 2014, **4**, 42577-42580.
31. Z. Jin, *Acta Botanica Yunnanica* 1999, **21**, 296-302.

297 **Table List**

Table 1 Overview of the sequencing results of the bands stabbed from the DGGE profiles.

Band	Accession	Name	Organism	Similarity
1	CP007391	*Escherichia coli*	*Proteobacteria*, *Gammaproteobacteria*, *Enterobacteriales*, *Enterobacteriaceae*	100%
2	EF668606	*Geobacteraceae* sp.	*Proteobacteria*, *Deltaproteobacteria*, *Desulfuromonadales*	98%
3	FJ440032	UF-1	Uncultured bacterium (*Firmicutes*, environmental sample)	98%
4	FN548084	UF-2	Uncultured bacterium (*Firmicutes*, environmental sample)	97%
5	JN221495	*Escherichia* sp.	*Proteobacteria*, *Gammaproteobacteria*, *Enterobacteriales*, *Enterobacteriaceae*	100%
6	CP001383	*Shigella*	*Proteobacteria*, *Gammaproteobacteria*, *Enterobacteriales*, *Enterobacteriaceae*	99%
7	JF344166	UG-1	*Proteobacteria*, *Gammaproteobacteria*	96%
8	KF767890	*Escherichia* sp.	*Proteobacteria*, *Gammaproteobacteria*, *Enterobacteriales*, *Enterobacteriaceae*	99%
9	GU477928	UR-1	Uncultured bacterium (RDX Degrading Microorganisms)	94%
10	KF851241	*Escherichia* sp.	*Proteobacteria*, *Gammaproteobacteria*, *Enterobacteriales*, *Enterobacteriaceae*	100%
11	HQ857728	*Salinimicrobium*	*Bacteroidetes*, *Flavobacteriia*, *Flavobacteriales*, *Flavobacteriaceae*	92%
12	KF851241	*Escherichia* sp.	*Proteobacteria*, *Gammaproteobacteria*, *Enterobacteriales*, *Enterobacteriaceae*	100%
13	DQ768632	*Alcanivorax*	*Proteobacteria*, *Gammaproteobacteria*, *Oceanospirillales*, *Alcanivoracaceae*	100%

298 **Figure Captions**

299 **Figure 1** Schematics of the soil microbial fuel cell (SMFC) (a) and the sectional
300 drawing (b). The circles and the star shaped symbols represent water and soil. SL1,
301 SL2, SL3 and SL4 indicate layer 1, layer 2, layer 3 and layer 4 of soil respectively.

302 **Figure 2** Voltage generation and charge output of the SMFC.

303 **Figure 3** Contents and net degradation rates of PAHs in soils from natural attenuation
304 (NA, disconnected control) and the closed circuit (CC) reactors (a) and contents of
305 PAHs in each layer of CC (b).

306 **Figure 4** Contents and net degradation rates of *n*-alkanes in NA and closed circuit
307 reactors (a) and each layer of CC (b-f).

308 **Figure 5** DGGE fingerprint (a), Shannon-Wiener Index, Uniformity Index and
309 Richness of NA and CC.

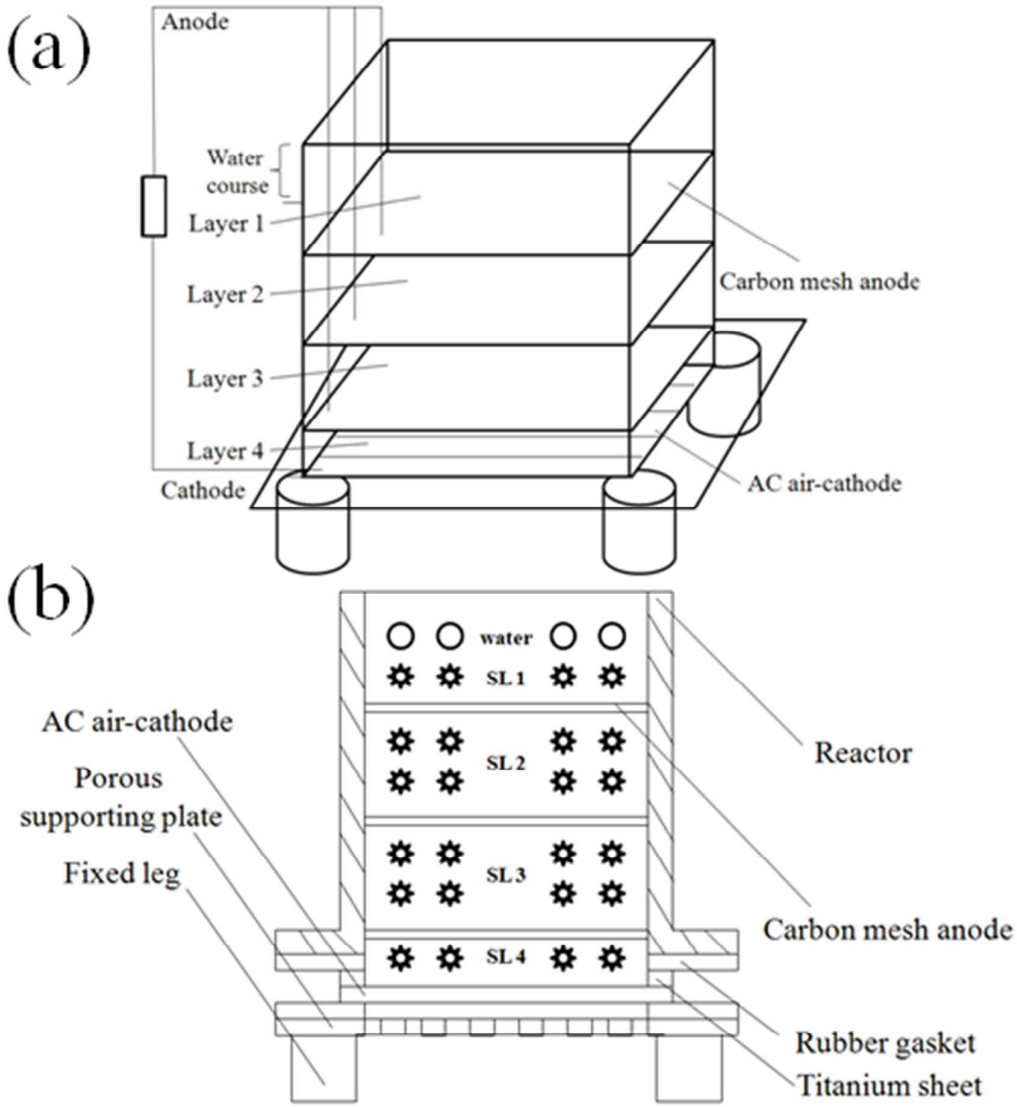

310

311 Figure 1

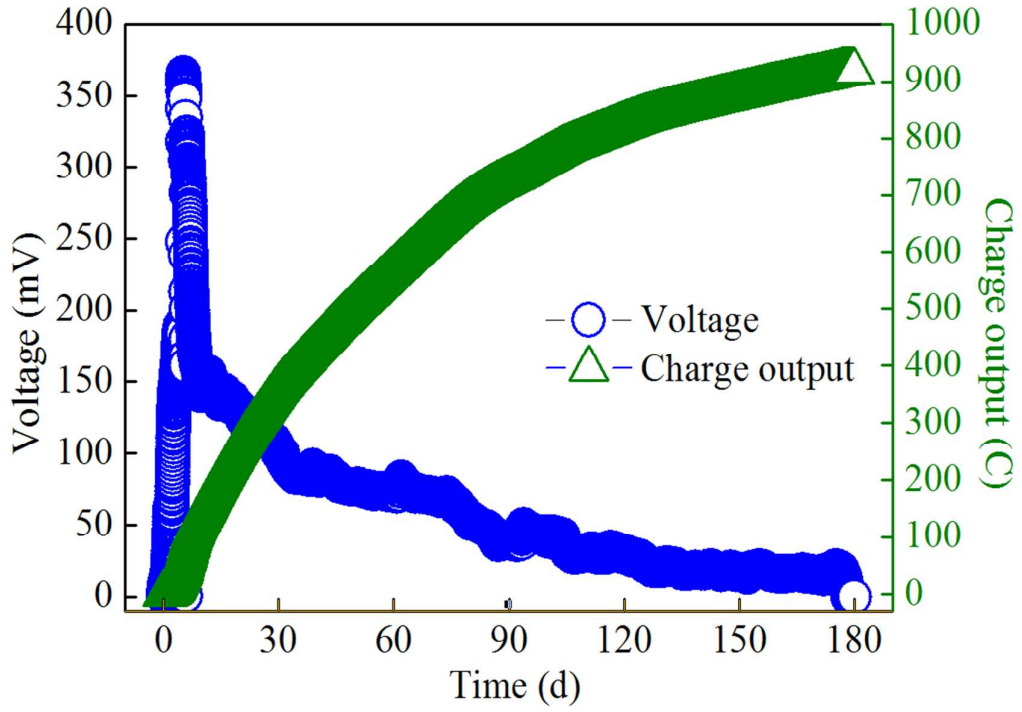

312

313 Figure 2

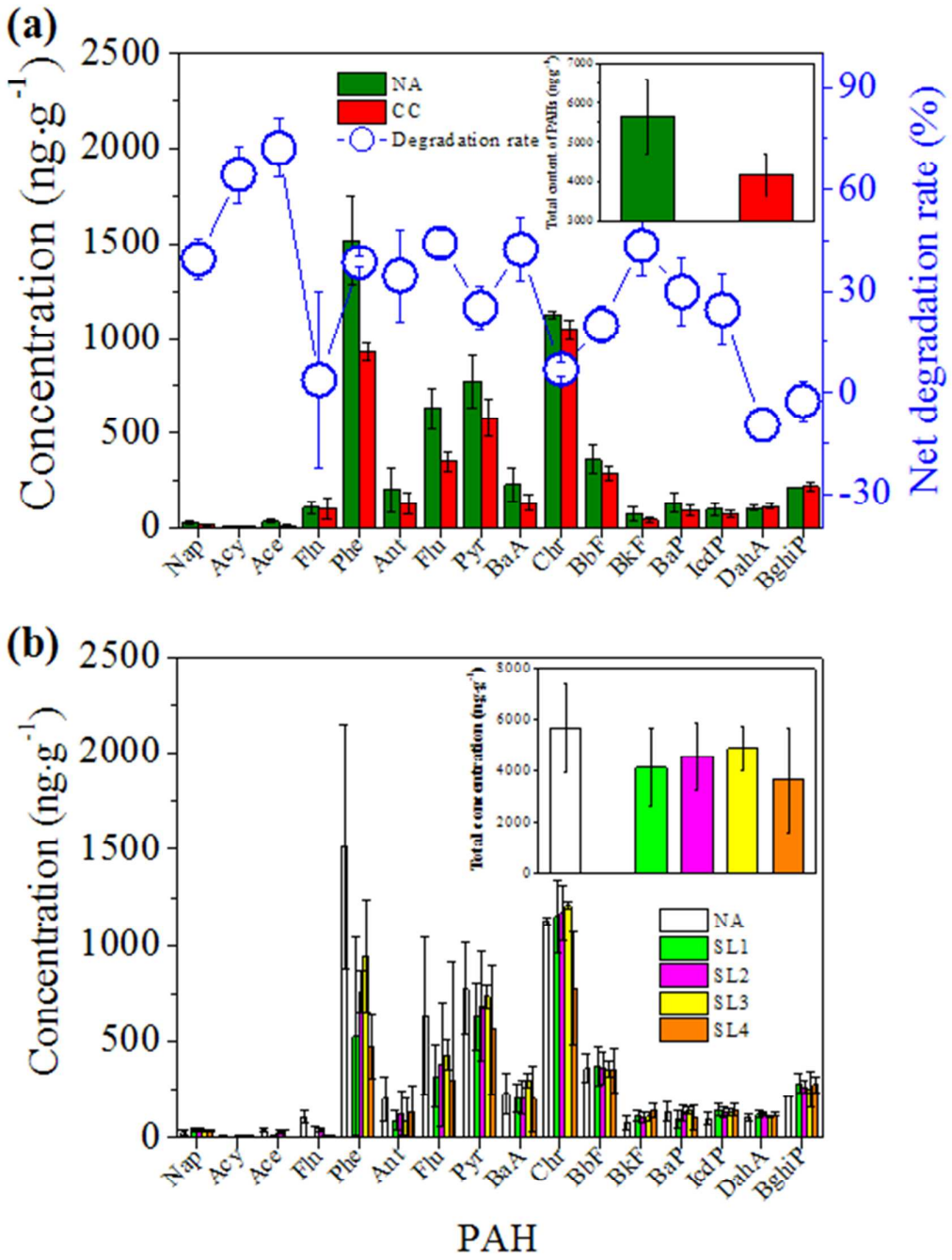

314

315 Figure 3

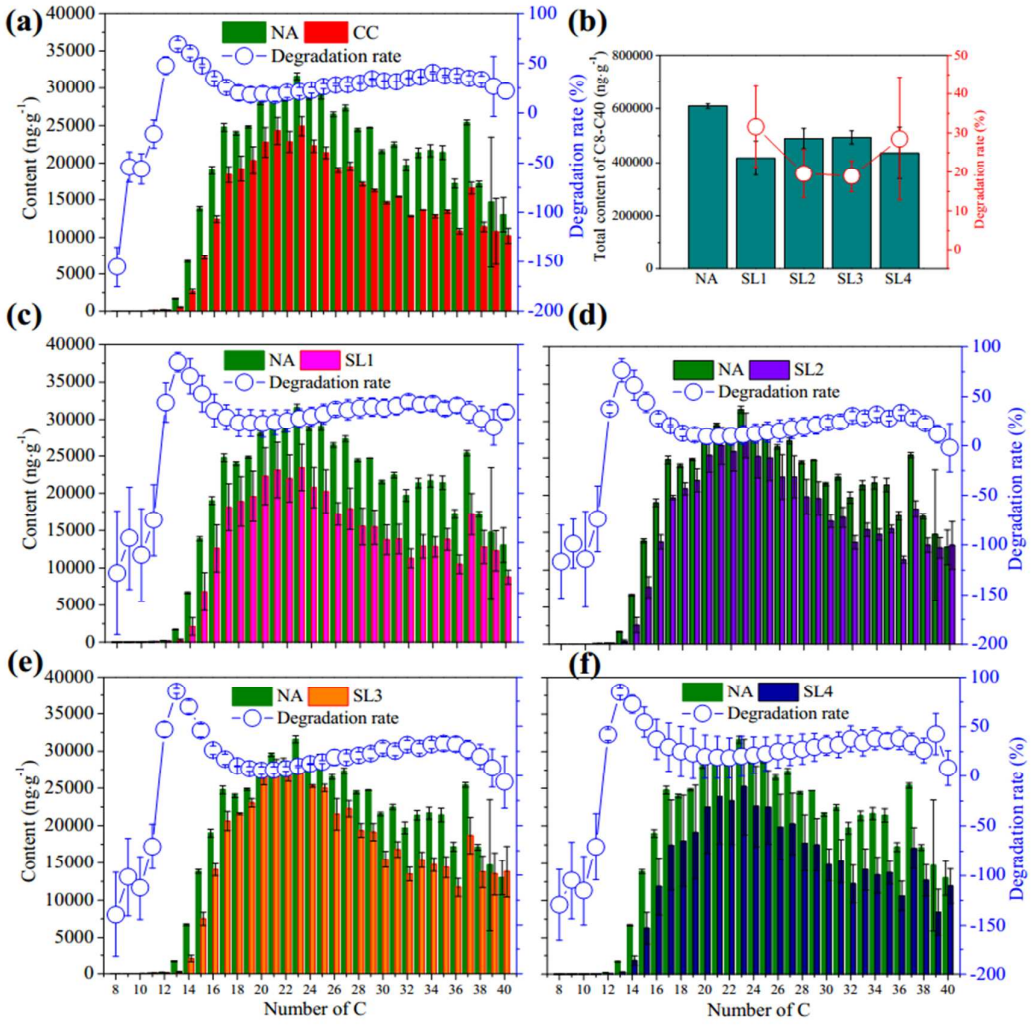

316

317 Figure 4

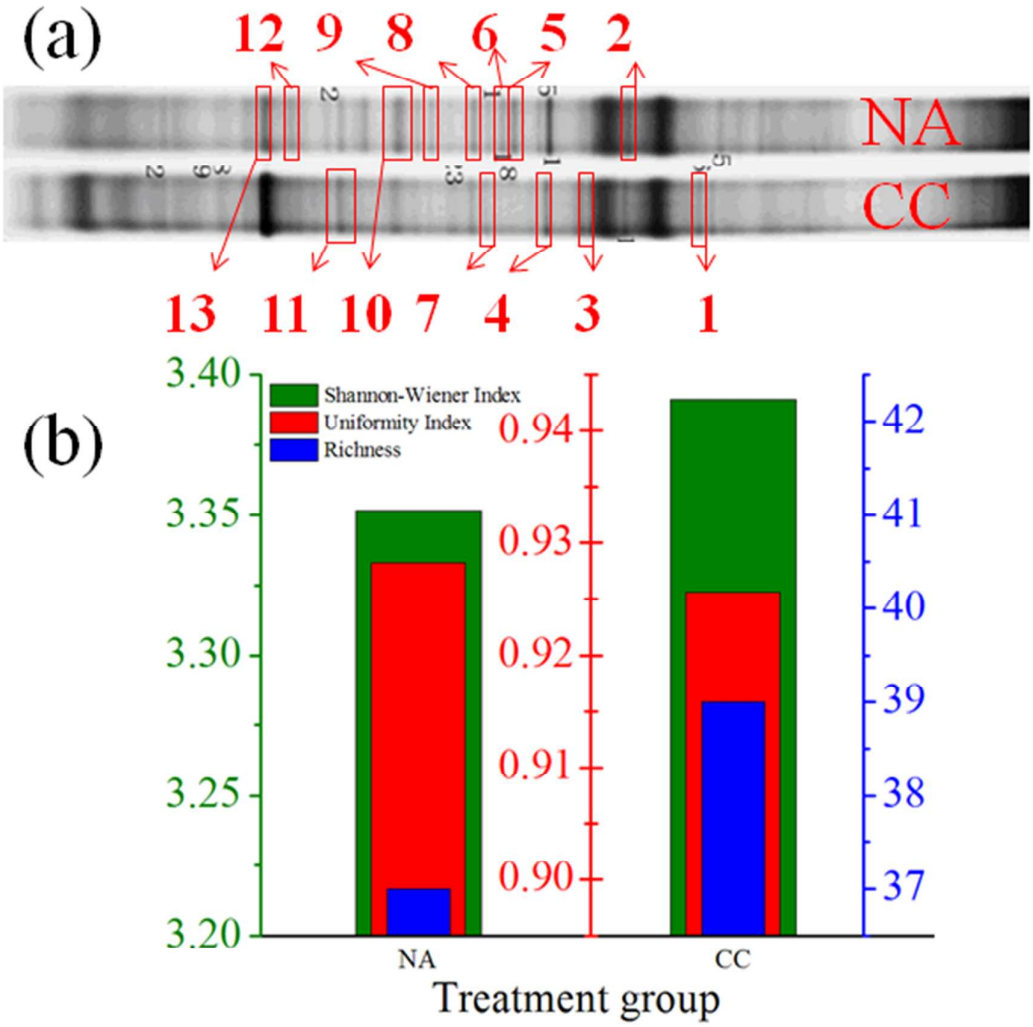

318

319 Figure 5